



The Role of Design-of-Experiments in Managing Flow in Compact Air Vehicle Inlets

Bernhard H. Anderson
Glenn Research Center, Cleveland, Ohio

Daniel N. Miller
Lockheed Martin Aerospace Company, Fort Worth, Texas

Marvin C. Gridley
Wright Patterson Air Force Base, Dayton, Ohio

Johan Agrell
Swedish Defence Research Agency, Bromma, Sweden

The NASA STI Program Office . . . in Profile

Since its founding, NASA has been dedicated to the advancement of aeronautics and space science. The NASA Scientific and Technical Information (STI) Program Office plays a key part in helping NASA maintain this important role.

The NASA STI Program Office is operated by Langley Research Center, the Lead Center for NASA's scientific and technical information. The NASA STI Program Office provides access to the NASA STI Database, the largest collection of aeronautical and space science STI in the world. The Program Office is also NASA's institutional mechanism for disseminating the results of its research and development activities. These results are published by NASA in the NASA STI Report Series, which includes the following report types:

- **TECHNICAL PUBLICATION.** Reports of completed research or a major significant phase of research that present the results of NASA programs and include extensive data or theoretical analysis. Includes compilations of significant scientific and technical data and information deemed to be of continuing reference value. NASA's counterpart of peer-reviewed formal professional papers but has less stringent limitations on manuscript length and extent of graphic presentations.
- **TECHNICAL MEMORANDUM.** Scientific and technical findings that are preliminary or of specialized interest, e.g., quick release reports, working papers, and bibliographies that contain minimal annotation. Does not contain extensive analysis.
- **CONTRACTOR REPORT.** Scientific and technical findings by NASA-sponsored contractors and grantees.

- **CONFERENCE PUBLICATION.** Collected papers from scientific and technical conferences, symposia, seminars, or other meetings sponsored or cosponsored by NASA.
- **SPECIAL PUBLICATION.** Scientific, technical, or historical information from NASA programs, projects, and missions, often concerned with subjects having substantial public interest.
- **TECHNICAL TRANSLATION.** English-language translations of foreign scientific and technical material pertinent to NASA's mission.

Specialized services that complement the STI Program Office's diverse offerings include creating custom thesauri, building customized databases, organizing and publishing research results . . . even providing videos.

For more information about the NASA STI Program Office, see the following:

- Access the NASA STI Program Home Page at <http://www.sti.nasa.gov>
- E-mail your question via the Internet to help@sti.nasa.gov
- Fax your question to the NASA Access Help Desk at 301-621-0134
- Telephone the NASA Access Help Desk at 301-621-0390
- Write to:
NASA Access Help Desk
NASA Center for Aerospace Information
7121 Standard Drive
Hanover, MD 21076



The Role of Design-of-Experiments in Managing Flow in Compact Air Vehicle Inlets

Bernhard H. Anderson
Glenn Research Center, Cleveland, Ohio

Daniel N. Miller
Lockheed Martin Aerospace Company, Fort Worth, Texas

Marvin C. Gridley
Wright Patterson Air Force Base, Dayton, Ohio

Johan Agrell
Swedish Defence Research Agency, Bromma, Sweden

Prepared for the
Vehicle Propulsion Integration Symposium
sponsored by the NATO Research and Technology Agency
Warsaw, Poland, October 6–9, 2003

National Aeronautics and
Space Administration

Glenn Research Center

The Propulsion and Power Program at
NASA Glenn Research Center sponsored this work.

Available from

NASA Center for Aerospace Information
7121 Standard Drive
Hanover, MD 21076

National Technical Information Service
5285 Port Royal Road
Springfield, VA 22100

Available electronically at <http://gltrs.grc.nasa.gov>

THE ROLE OF DESIGN-OF-EXPERIMENTS IN MANAGING FLOW IN COMPACT AIR VEHICLE INLETS

Bernhard H. Anderson
NASA Glenn Research Center, Cleveland, OH 44135
E-mail: anderson@brutus.grc.nasa.gov

Daniel N. Miller
Lockheed Martin Aerospace Company, Fort Worth, TX 76101
E-mail: Daniel.N.Miller@lmco.com

Marvin C. Gridley
Wright Patterson Air Force Base, Dayton, OH 45433
E-mail: Marvin.Gridley@wpafb.af.mil

Johan Agrell
Swedish Defence Research Agency, Bromma, Sweden
E-mail: alj@foi.se

ABSTRACT

It is the purpose of this study to demonstrate the viability and economy of *Design-of-Experiments* methodologies to arrive at microscale secondary flow control array designs that maintain optimal inlet performance over a wide range of the mission variables and to explore how these statistical methods provide a better understanding of the management of flow in compact air vehicle inlets. These statistical design concepts were used to investigate the *robustness* properties of “low unit strength” micro-effector arrays. “Low unit strength” micro-effectors are micro-vanes set at very low angles-of-incidence with very long chord lengths. They were designed to influence the near wall inlet flow over an extended streamwise distance, and their advantage lies in low total pressure loss and high effectiveness in managing engine face distortion. The term *robustness* is used in this paper in the same sense as it is used in the industrial problem solving community. It refers to minimizing the effects of the hard-to-control factors that influence the development of a product or process. In *Robustness Engineering*, the effects of the hard-to-control factors is often called “noise”, and the hard-to-control factors themselves are referred to as the environmental variables or sometimes as the Taguchi “noise” variables. Hence *Robust Optimization* refers to minimizing the effects of the environmental or “noise” variables on the development (design) of a product or process. In the management of flow in compact inlets, the environmental or “noise” variables can be identified with the mission variables. Therefore this paper formulates a statistical design methodology that minimizes the impact of variations in the mission variables on inlet performance and demonstrates that these statistical design concepts can lead to simpler inlet flow management systems.

INTRODUCTION

The current development strategy for combat air-vehicles is directed towards reduction in the Life-Cycle Cost (LCC) with little or no compromise to air-vehicle performance and survivability. This strategy has been extended to the aircraft component level, in particular, the engine inlet diffuser system. One method to reduce inlet system LCC is to reduce its structural weight and volume. Consequently, advanced combat inlet configurations are being made more compact (or shorter) to achieve weight and volume (and LCC) reduction. However, compact S-duct diffusers are characterized by high distortion and low pressure recovery, which are produced by extreme wall curvature and strong secondary flow gradients within the boundary layer. These characteristics are also further aggravated by maneuvering conditions. The requirement to highly integrate or embed the propulsion system into the airframe often leads to conformal inlet aperture shapes which do not lend themselves to high aerodynamic performance. These configurations also present a challenging environment for both fan/compressor surge margin and aeromechanical vibration. Interest in High Cycle Fatigue (HCF) research by the US aerospace community has been spurred by discrepancies between the expected durability of engine components compared to that actually experienced in the field. Recognizing that inlet distortion is a forcing function for vibration in the fan components, methods for increasing HCF Life Expectancy can be combined with techniques for inlet recovery and engine face distortion management. Therefore, to enable acceptable performance levels in such advanced, compact inlet diffuser configurations, microscale secondary flow control (MSFC) methods are being developed to manage the recovery, distortion, and HCF aspects of distortion.⁽¹⁾⁻⁽²⁾

One of the most difficult tasks in the design of a MSFC array for optimal inlet operation is arriving at the geometric placement, arrangement, number, size and orientation of the effector devices within the inlet duct to achieve optimal performance. These effector devices can be either mechanical (positive displacement) or fluidic. This task is complicated not only by the large number of possible design variables available to the aerodynamicist but also by the number of decision parameters that are brought into the design process. By including the HCF effects in the inlet design process, the aerodynamicist has a total of seven individual response variables that measure various aspects of inlet performance. These include the inlet total pressure recovery, the inlet total pressure recovery distortion at the engine face and the first five Fourier harmonic 1/2-amplitudes contained in the engine face distortion pattern. Each of these responses must be maximized, minimized, constrained or unconstrained while searching for the optimal combination of primary design variable values that satisfy the mission requirements. The design task is further complicated by the existence of hard-to-control factors that affect inlet performance, i.e. the mission variables. The mission variables that cause the off-design penalty are, for example, inlet throat Mach number (engine corrected weight flow), angle-of-incidence and angle-of-yaw. While the aerodynamicist does not know how the pilot is ultimately going to fly the aircraft, it is known how the mission variables affect inlet performance under wind tunnel conditions. Traditionally, tolerance or robustness to the mission variables was accomplished only after the parameter design was completed, usually by accepting whatever off-design performance was delivered by the newly designed inlet system. Numerical optimization procedures that have been successful with some aerodynamics problems give little assistance to designing robust inlets since they are point-design procedures, usually with only one decision parameter. However, there is a branch of statistical Design-of-Experiments (DOE) methodology which integrates both traditional *Response Surface Methods* (RSM) and *Robust Optimization Concepts* (ROC) into a single optimization procedure. It presents new potential for further reduction of *total quality cost* over the traditional design approach.

Taguchi⁽³⁾ coined the term Robust Parameter Design to describe an approach to industrial problem solving whereby the product variation is reduced by choosing levels of the control factors (design parameters) that make the product insensitive to the changes in the noise factors that represent sources of variations. These noise factors in industrial design are often the environmental variables such as temperature and humidity, properties of the material, and product aging. In some applications, the factors measure how the consumer uses or handles the product. In the aerodynamic design of inlet systems, there is an analogous situation to the industrial design problem. As mentioned above, the design of inlet systems is usually accomplished at the cruise condition (the on-design condition) while variations from the cruise condition are considered as an off-design penalty. Because the mission variables cause variation from on-design performance, they can be identified with the noise or environmental variables in the analogous industrial design problem. Likewise, how the pilot flies the aircraft can be identified with how the consumer uses or handles the product. In the industrial problem, researchers must be able to control the environmental variables in a laboratory environment, even though they cannot be controlled at the production level or in the field. Likewise, the aerodynamic researcher can indeed control the mission variables in the wind tunnel environment, however these variables cannot be controlled in flight (in the field). By making the analogy between the industrial design problem and the aerodynamic design problem, *Robust Optimization Concepts* developed for industrial problem solving can be adapted to the design of inlet systems⁽⁴⁾, and in particular, design of optimal robust microscale secondary flow control arrays⁽⁵⁾⁻⁽⁶⁾ which can simplify the inlet flow management system.

NOMENCLATURE

AIP	Aerodynamic Interface Plane	R	Inlet Radius
c	Effector Chord Length	R _{cl}	Centerline Radius
CCF	Central Composite Face-Centered	R _{ef}	Engine Face Radius
CFD	Computational Fluid Dynamics	R _{thr}	Inlet Throat Radius
D	Engine Face Diameter	ROC	Robust Optimization Concepts
DC60	Circumferential Distortion Descriptor	Re	Reynold Number per ft
DOE	Design of Experiments	RSM	Response Surface Methodology
h	Effector Blade Height	UAV	Unmanned Air Vehicle
HCF	High Cycle Fatigue	UCAV	Unmanned Combact Air Vehicle
Fk/2	k th Fourier Harmonic 1/2-Amplitude	X _{cl}	Axial Distance
FM/2	Mean Fourier Harmonic 1/2-Amplitude	Y _{i,j}	Generalized Response Variable
L	Inlet Diffuser Length	Y _{M,α}	Response Variable Summed over Mt and α
LCC	Life Cycle Costs	Z _{cl}	Centerline Offset Displacement
MSFC	microscale Secondary Flow Control	α	Inlet Angle-of-Incidence
Mt	Inlet Throat Mach Number	β	Effector Vane Angle-of-Incidence
n	Number of Effector Vanes per Band	ΔZ _{cl}	Inlet Centerline Offset
PFAVE	Average Inlet Total Pressure at AIP	γ	Inlet Angle-of-Yaw

RESULTS AND DISCUSSION

Baseline Flow in the Redesigned M2129 Inlet S-Duct

The redesigned M2129 inlet S-duct used in this study was considered similar to the original DERA/M2129 inlet S-duct defined by AGARD FDP Working Group 13 Test Case 3,⁽⁷⁾ using Lip No. 3 and Forward Extension No. 2. This inlet design was first proposed by Willmer, Smith and Goldsmith,⁽⁸⁾ and has been used extensively in the US and UK to explore inlet flow control array design. The centerline for the redesigned M2129 inlet is given by the equation

$$Z_{cl} = -\frac{\Delta Z_{cl}}{2} \left(1 - \cos \left(\pi \cdot \frac{X_{cl}}{L} \right) \right) \quad (1)$$

the radius distribution measured normal to the inlet centerline is given by the expression

$$\left(\frac{R_{cl} - R_{thr}}{R_{ef} - R_{thr}} \right) = 3 \left(1 - \frac{X_{cl}}{L} \right)^4 - 4 \left(1 - \frac{X_{cl}}{L} \right)^3 + 1 \quad (2)$$

where $R_{thr} = 2.5355$ inches, $R_{ef} = 3.0$ inches, $L = 15.0$ inches, and $\Delta Z_{cl} = 5.7809$ inches. The redesign of the M2129 inlet was such that the new inlet matches the static pressure gradients normally found in typical UAV or UCAV designs. Therefore, the new inlet is more compact than the original M2129 inlet S-duct. As a consequence, supersonic flow will develop in this inlet when the inlet throat Mach number increases much above 0.70.

Inlet Flow Control Array Design

To manage the flow in the redesigned M2129 inlet S-duct, a single band array arrangement of microscale effectors was placed in the upstream section near the inlet throat. See Figures (1). These microscale effectors were micro-vanes, the largest height being about the average height of the momentum layer just downstream of the inlet throat or about 2.0 mm. The purpose of these micro-vanes was to create a set of co-rotating vortices that would quickly merge to form a thin layer of secondary flow that will counter the formation of the passage vortex pair. Since the height of the vane effectors were limited to 2.0 mm, a single-band arrangement of micro-vanes set at 5.0° angle-of-incidence was chosen to investigate the enhancing effect of increasing the vane chord length on distortion management, i.e. allowing the array design to influence the inlet flow over an extended streamwise distance for a design advantage

The DOE approach followed directly from the objectives of the study and are reflected in the layout of the design factors listed in Table (1). The factor variables were the number of vane effector units (n), the micro-vane effector height (h), the micro-vane chord length (c), the inlet throat Mach number (Mt), and the inlet angle-of-incidence (α). Strictly speaking, the inlet throat Mach number and angle-of-incidence are mission variables and, therefore, the noise factors that belonged with the environmental variables, i.e. the outer array in a traditional Taguchi-style *Robust Parameter Design*. However, in this study, the throat Mach number and inlet angle-of-incidence were combined into the statistical DOE matrix with the control factors. This is called a combined DOE matrix array, which allowed greater economy than the traditional Taguchi approach⁽³⁾. The robust nature of the throat Mach number and inlet angle-of-incidence was investigated during the analysis phase of the data. Table (2) shows the variables that were held constant during this study. They include the effector vane thickness (t), the geometric angle-of-incidence of the micro vanes (β), the inlet operating total pressure (Pt) and temperature (Tt), and the inlet angle-of-yaw (γ). Table (3) displays the response variables for this study. They include the inlet total pressure recovery (PFAVE), the engine face distortion (DC60), and the first five Fourier harmonic 1/2-amplitudes of engine face distortion (F1/2, F2/2, F3/2, F4/2, and F5/2).

The DOE strategy selected was a Central Composite Face-Centered (CCF) DOE. This strategy resulted in 27 unique CFD experimental cases that are shown in Table (4). This DOE construct is called a combined array format because it contains both the factor (design) variables and the environmental (mission) variables. Notice that these DOE cases covered a substantial range of possible flow situations over a wide range of throat Mach numbers from 0.30 to 0.70, and angles-of-incidences from 0.0° to 20.0°. This particular DOE, like most DOE strategies, varied more than one factor at a time. Further, this layout of 27 cases permitted the estimation of both linear and curvilinear effects as well as two-factor interactive or synergistic effects among the DOE factors. This CCF DOE strategy is superior to the traditional approach where only changing one variable at a time does not permit the estimation of the two-factor interactions. It is also more economical at 27 runs than a full factorial approach where the number of experiments would be 3⁵ or 243 separate CFD cases. It is also more economical than a comparable Taguchi approach requiring 15 x 3 = 45 experiments.

A graphical representation of the Central Composite Face-Centered DOE used in the study is presented in Figure (2). The DOE cases are represented in this figure by the circular symbols, where the symbol

locations on the cube signify its factor value. This DOE is called a composite DOE because the organization of cases is composed of a fractional factorial part and a quadratic part. The fractional factorial part of the DOE is composed of one-half of the 2^5 possible cases, i.e. 32 possible factorial cases, which are represented by the eight corner locations in each of the four corner-cubes in Figure (2). Because only half the number of possible factorial cases are actually used in this DOE format (circular symbols), the layout is called a 1/2-fractional of the full factorial and is composed of 2^{5-1} cases, or 16 separate CFD runs. The remaining cases in Figure (2) are the quadratic part of the DOE. The quadratic cases allow for the evaluation of the curvilinear effects. All together, there are a total of 27 cases in a Central Composite Face-Centered DOE with five factor variables. Notice the balanced layout of cases in Figure (2). The factor variables are represented by the axes of the individual cubes, while the environmental (mission) variables are represented by the different cubes. This layout of cases represents the smallest number of CCF DOE cases that allows for the evaluation of linear and curvilinear effects as well as all two-factor interactive or synergistic effects.

Each of the 27 cases in Table (4) was run with a Reynolds-averaged Navier-Stokes code⁽⁹⁾ that allowed for numerical simulation of micro-vane effectors without the need to physically embed the vane effectors within the CFD grid structure. However, for the present study the individual vanes were incorporated into the half cylindrical grid structure. These micro-vanes all had a thickness of 0.138 mm. See Table (2). The computational grid was developed such that it reasonably resolved the boundary layer development on both the suction and pressure surfaces of each micro-vane in the array. Because wall functions were used in the calculations, the grid resolution for the individual micro-vanes was simplified. However, the boundary layer along the micro-vane edges was assumed to be negligible, and therefore not resolved in the computational grid. The half cylindrical grid structure was composed of three blocks: an upstream block, an effector section containing the micro-vanes, and a downstream block. See Figures (1). The computational half-plane grid varied in total number of mesh points from about 950,000 to 1,150,000 depending on the micro-vane configuration. All CFD calculations were accomplished assuming half cylindrical symmetry. A two-equation k- ϵ turbulence model was used in this study. The model consists of transport equation for the turbulent kinetic energy and turbulent length scale. The model includes a near-wall model and compressible corrections for high speed flows. To introduce an angle-of-incidence (α -disturbance) into the flow analysis, the condition was imposed that the initial station have an angle-of-incidence component that approximated the measured angle-of-incidence flow field⁽¹⁰⁾.

Optimal Flow Control Over the Mission Variable Range

To illustrate the potential of RSM and *Robust Optimization Concepts* to design and optimize MSFC arrays, three mission strategies were considered for the subject inlet, namely (1) Maximum Performance, (2) Maximum Engine Stability, and (3) Maximum HCF Life Expectancy. The Maximum Performance mission minimized the inlet total pressure losses, the Maximum Engine Stability mission minimized the engine face distortion, while the Maximum HCF Life Expectancy mission minimized the mean of the first five Fourier harmonic amplitudes, i.e. “collectively” reduced all the harmonic 1/2-amplitudes of engine face distortion. Each of the mission strategies was subject to a low engine face distortion constraint, i.e. $DC60 \leq 0.10$, which is a level acceptable for commercial engines, and a constraint on each individual Fourier harmonic 1/2-amplitudes: $Fk/2 \leq 0.015$, $k = 1, 2, \dots, 5$. For each of three mission strategies, i.e. Maximum Performance, Maximum Engine Stability, and Maximum HCF Life Expectancy mission, an “Optimal Robust” (open loop control) and an “Optimal Adaptive” (closed loop control) array were designed to operate over an inlet throat Mach number range from 0.30 to 0.70, and angle-of-incidence range from 0.0° to 20.0° . The “Optimal Robust” array arrived at a single MSFC array which operated optimally over the entire throat Mach number and angle-of-incidence range (open loop control). The “Optimal Adaptive” array optimized all the design parameters at each throat Mach number and angle-of-incidence. Thus the “Optimal Adaptive” array would require a closed loop control system to sense a proper signal for each effector and modify that effector device, whether mechanical or fluidic, for optimal inlet performance. The inlet throat Mach number and angle-of incidence range were the Taguchi noise or environmental variables over which each optimal array had to be robust. A detailed description of the robust methodology used in the present study appears in Anderson and Keller,⁽⁴⁾ and is termed the “Lower Order” method, while a lengthy comparison between the “Lower Order”, Taguchi and an alternative “High Order” method appears in Anderson and Keller.⁽⁵⁾

Maximum Performance Mission - To obtain the “Optimal Adaptive” Maximum Performance optimal array designs, the inlet duct losses:

$$Y_{i,j} = (1 - PFAVE)_{i,j} \quad (3)$$

where minimized at each of the N_M values of inlet throat Mach numbers and each of the N_α angles-of-incidence to obtained the optimal array corresponding to that inlet operating condition. In a similar manner, the “Optimal Robust” Maximum Performance array design was determined through a search process to locate that array geometry that minimized the decision parameter:

$$Y_{M, \alpha} = \frac{1}{N_M} \sum_{i=1}^{N_M} \frac{1}{N_\alpha} \sum_{j=1}^{N_\alpha} (1 - PFAVE)_{i,j} \quad (4)$$

where N_M is the number of throat Mach number conditions in the set from Mt = 0.30 to 0.70, and N_α is the number angles-of-incidence in the set from $\alpha = 0.0$ to 20.0° . Both the “Optimal Adaptive” and “Optimal Robust” were both subject to the engine face distortion constraint that

$$DC60 \leq 0.10 \quad (5)$$

and the individual Fourier harmonic 1/2-amplitudes of distortion constraint to

$$\frac{Fk}{2} \leq 0.015 \quad (6)$$

The Optimal Robust Maximum array design was determined through a search process to have factor values of $n = 22$, $h = 1.95$ mm, and $c = 72.0$ mm. In order to validate the DOE prediction results, a set of nine cases was run using the “Optimal Robust” array design determined from the search procedure described. The Maximum Performance validation cases⁽⁶⁾ were organized as a full factorial array with the two mission variables at three levels each, i.e. 3^2 experiments.

Comparisons between the performance results of the “Optimal Robust” and “Optimal Adaptive” arrays for the Maximum Performance inlet mission are shown in Figure (3). Also presented in Figures (3) is the inlet baseline performance at an inlet throat Mach number of 0.70 for each response. It is apparent from Figure (3) that flow control was able to increase total pressure recovery substantially above the baseline flow at 0.70 inlet throat Mach number. This was not the case for the high strength micro-vane effector units.⁽⁴⁾⁻⁽⁵⁾ The “Optimal Robust” and “Optimal Adaptive” arrays provided essentially the same performance over the inlet throat Mach number range for 0.30 to 0.70 and angle-of-incidence range of 0° to 20° . This is not surprising, since there exists experimental data⁽¹⁰⁾ that demonstrate that a fixed secondary flow control array optimally designed can provide essentially the same low DC60 distortion level, i.e. $DC60 \leq 0.10$, over a substantial angle-of-incidence range. Secondary flow control in inlets is inherently robust, provided it is optimally designed. In addition, “Optimal Robust” and “Optimal Adaptive” arrays reduced all the Fourier harmonic 1/2-amplitudes to a value of 0.01 or below, which is extremely low. Although a correlation between engine face distortion and the Fourier harmonic 1/2-amplitudes can not be established, reducing the Fourier harmonic 1/2-amplitudes is essentially the same at reducing the engine face circumferential distortion.

Maximum Engine Stability Mission - To obtain the “Optimal Adaptive” Maximum Engine Stability array designs, a search was made over the factor variable space to locate that array geometry that minimized the decision parameter:

$$Y_{i,j} = (DC60)_{i,j} \quad (7)$$

at each throat of the N_M inlet throat Mach numbers and each of the N_α inlet angles-of-incidence. In a similar manner, the “Optimal Robust” Maximum Engine Stability array design was determined through a search process to locate that array geometry that minimized the decision parameter:

$$Y_{M, \alpha} = \frac{1}{N_M} \sum_{j=1}^{N_M} \frac{1}{N_\alpha} \sum_{i=1}^{N_\alpha} (DC60)_{i,j} \quad (8)$$

where N_M is the number of throat Mach number conditions in the set from Mt = 0.30 to 0.70, and N_α is the number of angles-of-incidence in the set from $\alpha = 0.0$ to 20.0° . Both the “Optimal Adaptive” and “Optimal Robust” arrays were both subject to the constraint that

$$\frac{Fk}{2} \leq 0.015 \quad (9)$$

while no constraint was placed on the inlet total pressure recovery (PFAVE). The Optimal Robust Engine Stability array design was determined through a search process to have factor values of $n = 24$, $h = 2.0$ mm, and $c = 70.2$ mm. In order to validate the DOE prediction results, a set of nine cases was run using the “Optimal Robust” array design determined from the search procedure described. These validation cases⁽⁶⁾ were organized as a full factorial array with the two mission variables at three levels each, i.e. 3^2 experiments.

Maximum HCF Life Expectancy Mission - The “Optimal Adaptive” Maximum HCF Life Expectancy MSFC array was determined through a search process over the factor variable space to locate that array geometry that minimized the mean of the first five Fourier harmonic 1/2-amplitudes of engine face distortion, i.e

$$Y_{i,j} = \frac{1}{5} \sum_{k=1}^5 \left(\frac{Fk}{2} \right)_{i,j} \quad (10)$$

at each of the N_M inlet throat Mach numbers and each of the N_α inlet angles-of-incidence. The “Optimal Robust” Maximum HCF Life Expectancy MSFC array was also determined through a search process over the factor variable space to locate that array geometry that minimized the decision parameter:

$$Y_{M,\alpha} = \frac{1}{N_M} \sum_{i=1}^{N_M} \frac{1}{N_\alpha} \sum_{j=1}^{N_\alpha} \frac{1}{5} \sum_{k=1}^5 \left(\frac{Fk}{2} \right)_{i,j} \quad (11)$$

where N_M is the number of throat Mach number conditions in the set from $Mt = 0.30$ to 0.70 , and N_α is the number angles-of-incidence in the set from $\alpha = 0.0$ to 20.0° . Both the “Optimal Adaptive” and “Optimal Robust” arrays designs were both subject to the engine face distortion constraint that

$$DC60 \leq 0.10 \quad (12)$$

and each Fourier harmonic 1/2-amplitude satisfy the expression:

$$\frac{Fk}{2} \leq 0.015 \quad (13)$$

The Optimal Robust HCF Life Expectancy array design was determined through a search process to have factor values of $n = 19$, $h = 1.70$ mm, and $c = 63.0$ mm. In order to validate the DOE prediction results, a set of nine cases was run using the “Optimal Robust” array design determined from the search procedure described. The Maximum HCF Life Expectancy validation cases⁽⁶⁾ were likewise organized as a full factorial array with the two mission variables at three levels each, i.e. 3^2 experiments.

Statistical Comparison of CFD Analysis and DOE Predictions

Presented in Anderson, Baust, and Agrell⁽⁶⁾ are the results of the statistical comparison between the CDF analysis and DOE predictions for the Maximum Performance, Maximum Engine Stability, and Maximum HCF Life Expectancy mission validation cases. These comparisons were made over the range of throat Mach Numbers from 0.30 to 0.70 and inlet angle-of-incidences from 0° to 20.0° . In general, the number of incidences when the comparisons were statistically different was somewhat above 5%, which is remarkably good. All the cases in which a statistical difference were indicated involved in the evaluation of the Fourier harmonic 1/2-amplitudes of distortion. In these particular cases, the differences between the CFD analysis and DOE prediction were too small to be of practical significance, i.e. they could not be experimentally measured. This indicates that the DOE prediction results were not statistically different from the CFD analysis results (i.e. the CFD analysis predictions fell within the 95% confidence interval of the DOE performance predictions). It also indicated that the optimal arrays determined by the DOE models were a statistically valid optima when compared to the actual CFD array analyses. The accuracy of the response surfaces determined from the DOE analysis was therefore more than adequate for use in determining an array optimum and for conceptual studies on the inlet-engine flow management system.

Comparison of the Optimal Robust Array Designs

Comparison of the performance of the three “Optimal Robust” array designs, i.e. the Maximum Performance, Maximum Engine Stability, and Maximum HCF Life Expectancy mission designs, are shown in Figures (4) through (8) at a throat Mach numbers of 0.30 , 0.50 , and 0.70 and an inlet angles-of-incidence of 0.0° , 10.0° and 20.0° . These figures also include the baseline inlet performance, i.e. the performance of the redesigned M2129 inlet S-duct without flow control. The low strength effector units used in these designs achieved a substantial improvement in inlet total pressure recovery (PFAVE) over the baseline performance. See Figure (9). This differs from the performance of the high strength effector units which never increased the inlet total pressure recovery above the baseline value⁽⁴⁾. Excellent engine face distortion characteristics were also achieved with the low strength effector units as shown in Figure (10). Although very low engine face distortion was also achieved with the high strength effector units⁽⁴⁾, the overall array reductions were substantially greater for the present designs. Presented in Figure (11) is a comparison of the first five Fourier harmonic 1/2-amplitudes for the three “Optimal Robust” array designs with the baseline inlet characteristics. Minimizing the mean of the first five Fourier harmonic 1/2-amplitudes resulted in a substantial reduction in the amplitudes of the first three harmonics 1/2-amplitudes, and very low amplitudes for the fourth and fifth harmonic components.

By visually comparing the performance of the three “Optimal Robust” arrays designs presented in Figures (10) through (12), it is obvious that they are remarkably similar. This similarity can be established

objectively by a statistical comparison between the optimal CFD performance validations presented in Anderson, Baust, and Agrell.⁽⁶⁾ Since each of the three (3) sets of nine (9) CFD validation cases listed in these tables were run at the same conditions of throat Mach number and inlet angle-of-incidence, they represent three (3) sets of nine (9) matched pairs of CFD observations. The data in these tables have been ordered such that the differences in each of the nine (9) matched pairs of CFD observations can be tested as a paired t-test. In a paired t-test, the mean of the sample difference and the standard deviation of the sample difference is calculated and the following t-statistic determined:

$$t^* = \frac{\left| \frac{1}{N} \sum_{j=1}^N \Delta_j \right|}{\sqrt{\sum_{j=1}^n \frac{(\Delta_j - \bar{\Delta})^2}{(N-1)}}} \quad (14)$$

where $\Delta_j = (Y_1 - Y_2)_j$ is the difference of each of the N-pairs of the response variable in the two data sets.

In comparing the mean values from two data sets (1) and (2), if the expression

$$t^* < t(0.975, v_p) \quad (15)$$

is valid, the response values from the first data set are not statistically different from the response values from the second data set at the 95% confidence level. Likewise, the response values from the first data set are statistically different from the response values from the second data set at the 95% confidence level if the expression

$$t^* > t(0.975, v_p) \quad (16)$$

holds. The term v_p is the “pooled” degrees of freedom which, for a paired t-test, is given by the expression:

$$v_p = (N - 1) \quad (17)$$

and $t(0.975, v_p)$ is the 95% confidence t-value for v_p degrees of freedom.

The results of the paired t-test for the CFD validation cases are presented in Tables (10), (11) and (12). These evaluations have been organized as three sets of comparisons for two “Optimal Robust” mission array designs. In the first comparison, the Maximum Performance (data set 1) and Maximum Engine Stability (data set 2) mission cases are evaluated for the seven response variables. These comparisons are presented in Tables (10). In the second comparison the Maximum Performance (data set 1) and Maximum HCF Life Expectancy (data set 3) mission cases are evaluated, again for the same seven response variables. These comparisons are presented in Tables (11). Table (12) presents the results for the third set of comparisons, i.e. between the Maximum Engine Stability (data set 2) and Maximum HCF Life Expectancy (data set 3) mission cases for the same seven response variables. The seven response variables evaluated were the inlet total pressure recover (PFAVE), the engine face distortion (DC60), the first five Fourier harmonic 1/2-amplitudes of distortion (F1/2, F2/2, F3/2, F4/2, F5/2). The results of this study indicated that there were no statistical significant differences between the three sets of CFD validation cases at the 95% confidence level. Even though there are differences in the factor variables that define the “Optimal Robust” array designs, these factor differences did not translate into statistically significant inlet performance differences over the range of throat Mach Numbers from 0.30 to 0.70 and inlet angle-of-incidences from 0° to 20.0°.

CONCLUSIONS

The fundamental importance of Genichi Taguchi’s contribution to RSM over traditional design approaches lies in the idea that process and product sensitivity to their environment can be incorporated into the optimal statistical Design-of-Experiment and subsequent analysis of the data. The Taguchi noise factors that cause variability in industrial design are often the environmental variables, such as temperature and humidity, properties of the material, and product aging. In aerodynamic design, the Taguchi noise factors can be identified with the mission variables, since they produce variation from the design condition. Being able to include the mission variables directly into the inlet design process represents a major breakthrough in the area of aerodynamic design of inlets. The inlet system can now be designed to operate with optimal performance over a range of specified mission variables. Taguchi’s *Robust Parameter Design* method, however, may not be optimal in the design of secondary flow arrays for inlet systems because: (a) it loses information vital to the aerodynamicist and, (b) it is costly. Fortunately, the important aspects surrounding Taguchi’s approach to *Robust Parameter Design* can and have been incorporated into an alternate economical approach and adapted to the inlet design problem. This alternate inlet design method, using a combined array approach to economical *Robust Optimization Design*, had a significant run size savings over a traditional Taguchi approach, i.e. 27 CFD experiments as compared to 45 CFD experiments. The combined array DOE format, in which the factor (design) variables are included with the envi-

ronmental (mission) variables, allows for conceptual studies to be made on the inlet-engine control system to determine the most efficient and cost effective management system prior to any experimentation. These conceptual studies on the inlet-engine flow management system can not be made using Taguchi's *Robust Parameter Design* methodology.

To illustrate the potential of *Robust Optimization* methodology, three different mission strategies were considered for the subject inlet, namely (1) Maximum Performance, (2) Maximum Engine Stability, and (3) Maximum HCF Life Expectancy. The Maximum Performance mission minimized the inlet total pressure losses, the Maximum Engine Stability mission minimized the engine face distortion (DC60), while the Maximum HCF Life Expectancy mission minimized the mean of the first five Fourier harmonic amplitudes, i.e. "collectively" reduced all the harmonic 1/2-amplitudes of engine face distortion. Although the three "Optimal Robust" array designs were generated from three very different mission strategies, the performance achieved by these array designs were not statistically significantly different over the entire mission variable range. Hence one can draw overall conclusions with regard to microscale secondary flow control array design. Since each of the "Optimal Robust" array designs achieved near uniform engine face circumferential distortion, one can conclude that this condition represents the most robust operating state of the inlet. In addition, although there is no established correlation between the seven response variables tested in this study, it is clear that numerically optimizing the secondary flow array designs over the mission variable range drives all the response variables to their optimal levels. In Robust Optimization, therefore, the system is greatly simplified because the inlet response variables are collectively managed. Had the array not been numerically optimized, the response variables would have to have been individually managed, and the inlet management system would become far more complex.

In general, the performance differences between the "Optimal Adaptive" and "Optimal Robust" array designs were found to be marginal. This suggests, that "Optimal Robust" open loop array designs can be very competitive with "Optimal Adaptive" close loop designs. Thus the design concept of Robust Optimization, where the variability caused by the mission parameters is minimized, is achievable and valid. This design concept results in a simpler inlet management system as compared to closed-loop active feedback control. Under closed-loop active feedback control, the state of the inlet must be sensed and a corresponding reaction to that state must be implemented for each response variable. Taking advantage of the *Optimal Robustness* properties of microscale secondary flow control therefore can lead to simpler, more reliable and more cost effective inlet management systems.

REFERENCES

- (1) Anderson, B. H., Miller, D. M., Yagel, P. J., and Truax, P. P., "A Study of MEMS Flow Control for the Management of Engine Face Distortion in Compact Inlet Systems", FEDSM99-6920, 3rd ASME/JSME Joint Fluids Engineering Conference, San Francisco, CA, July 18-23, 1999.
- (2) Hamstra, J. W., Miller, D. N., Truax, P. P., Anderson, B. H., and Wendt, B. J., "Active Inlet Flow Control Technology Demonstration", ICAS-2000-6.11.2, 22nd International Congress of the Aeronautical Sciences, Harrogate, UK, August 27th-September 1st, 2000.
- (3) Taguchi, G and Wu, Y., "Introduction to Off-Line Quality Control," Central Quality Control Association, 1980.
- (4) Anderson, B. H. and Keller, D. J., "A Robust Design Methodology for Optimal Micro-Scale secondary Flow Control in Compact Inlet Diffusers", AIAA Paper No. 2002-0541, Jan. 2002.
- (5) Anderson, B. H. and Keller, D. J., "Robust Design Methodologies for Optimal Micro-Scale Secondary Flow Control in Compact Inlet Diffusers", NASA/TM-2001-211477, March 2001.
- (6) Anderson, B. H., Baust, H. D., and Agrell, J., "Management of Total Pressure Recovery, Distortion, and High Cycle Fatigue in Compact Air Vehicles Inlets", NASA/TM-2002-212000, Dec. 2002.
- (7) AGARD FTP Working Group 13, "Air Intakes for High Speed Vehicles", AR-270, September 1991.
- (8) Willmer, A. C., Brown, T. W. and Goldsmith, E. L., "Effects of Intake Geometry on Circular Pitot Intake Performance at Zero and Low Forward Speeds", Aerodynamics of Power Plant Installation, AGARD CP301, Paper 5, Toulouse, France, May 1981, pp 51-56.
- (9) Bender, E. E., Anderson, B. H., and Yagle, P. J., "Vortex Generator Modeling for Navier Stokes Code", FEDSM99-69219, 3rd ASME/JSME Joint Fluids Engineering Conference, San Francisco, CA, July 18-23, 1999.
- (10) Gibb, J. and Anderson, B. H., "Vortex Flow Control Applied to Aircraft Intake Ducts," Proceedings of the Royal Aeronautical Society Conf., High Lift and Separation Control, Paper No. 14, Bath, UK, March, 1995.

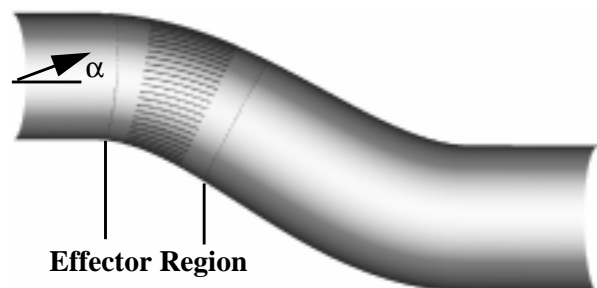


Figure (1): Location of effector region within inlet S-duct configuration

Factor	Range
Number of Vane Effectors, n	13 to 27
Effector Vane Height (mm), h	1.0 to 2.0
Effector Chord Length (mm), c	36.0 to 72.0
Inlet Throat Mach Number, Mt	0.30 to 0.70
Inlet Angle-of-Incidence (deg.), α	0.0 to 20.0

Table (1): Factor variables which establish the DOE design matrix.

Variable	Value
Effector Vane Thickness (mm), t	0.138
Vane Angle-of-Incidence (deg.), β	5.0
Inlet Total Pressure (lbs/ft ²), Pt	10506.0
Inlet Total Temperature (°R), Tt	517.0
Inlet Angle-of-Yaw (deg.), γ	0.0

Table (2): Variables held constant.

Response	Nomenclature
Engine Face Total Pressure Recovery	PEAVE
Engine Face Distortion	DC60
1st Fourier Harmonic 1/2-Amplitude	F1/2
2nd Fourier Harmonic 1/2-Amplitude	F2/2
3rd Fourier Harmonic 1/2-Amplitude	F3/2
4th Fourier Harmonic 1/2-Amplitude	F4/2
5th Fourier Harmonic 1/2-Amplitude	F5/2

Table (3): DOE response variables

Config.	n	h	c	Mt	α
nvg701	13	1.0	36.0	0.30	20.0
nvg702	27	1.0	36.0	0.30	0.0
nvg703	13	2.0	36.0	0.30	0.0
nvg704	27	2.0	36.0	0.30	20.0
nvg705	13	1.0	72.0	0.30	0.0
nvg706	27	1.0	72.0	0.30	20.0
nvg707	13	2.0	72.0	0.30	20.0
nvg708	27	2.0	72.0	0.30	0.0
nvg709	13	1.0	36.0	0.70	0.0
nvg710	27	1.0	36.0	0.70	20.0
nvg711	13	2.0	36.0	0.70	20.0
nvg712	27	2.0	36.0	0.70	0.0
nvg713	13	1.0	72.0	0.70	20.0
nvg714	27	1.0	72.0	0.70	0.0
nvg715	13	2.0	72.0	0.70	0.0
nvg716	27	2.0	72.0	0.70	20.0
nvg717	13	1.5	54.0	0.50	10.0
nvg718	27	1.5	54.0	0.50	10.0
nvg719	20	1.0	54.0	0.50	10.0
nvg720	20	2.0	54.0	0.50	10.0
nvg721	20	1.5	36.0	0.50	10.0
nvg722	20	1.5	72.0	0.50	10.0
nvg723	20	1.5	54.0	0.30	10.0
nvg724	20	1.5	54.0	0.70	10.0
nvg725	20	1.5	54.0	0.50	0.0
nvg726	20	1.5	54.0	0.50	20.0
nvg727	20	1.5	54.0	0.50	10.0

Table (4): “Lower Order” Central Composite Face-Centered (CCF) combined array DOE format involving factor (design) variables and environmental (mission) variables

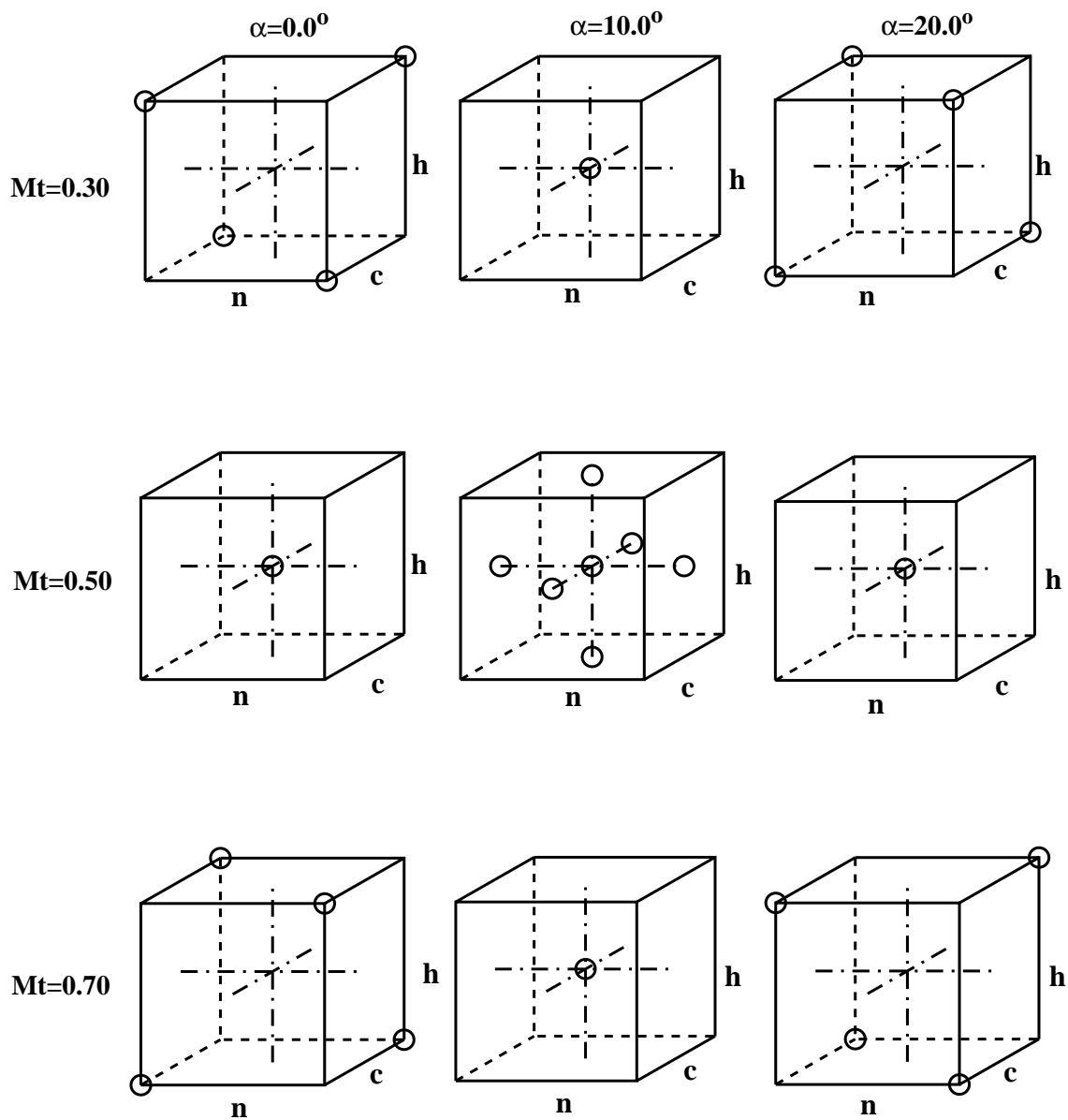
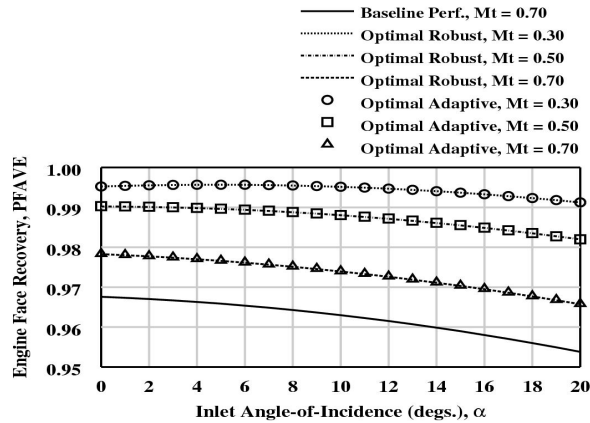
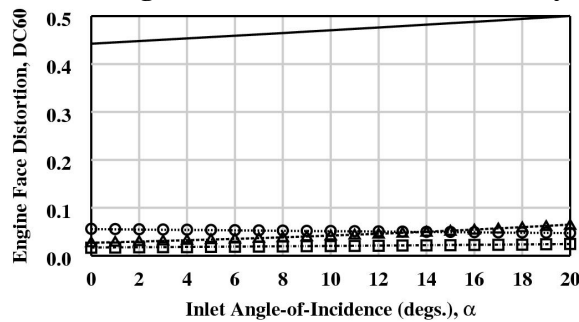


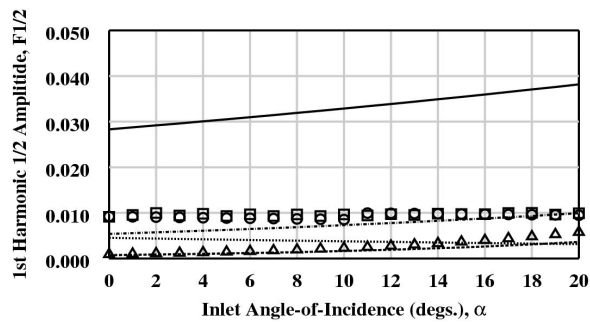
Figure (2): Graphical representation of the “Lower Order” Central Composite Face-Centered (CCF) combined array DOE format involving factor (design) variables and environmental (mission) variables.



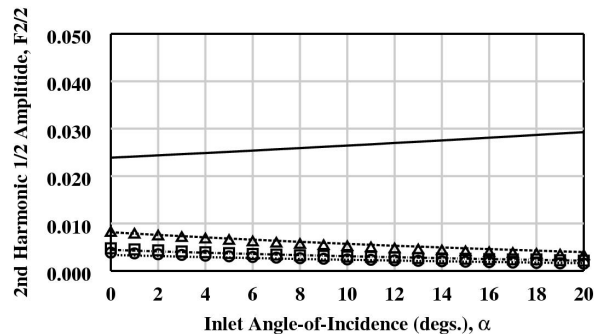
(a) Engine Face Total Pressure Recovery



(b) Engine Face DC60 Distortion

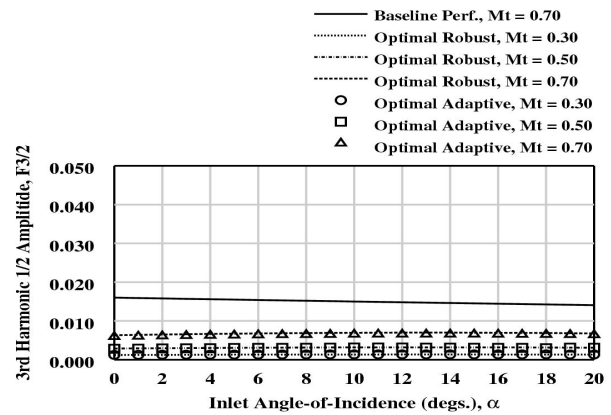


(c) 1st Fourier Harmonic 1/2 Amplitude

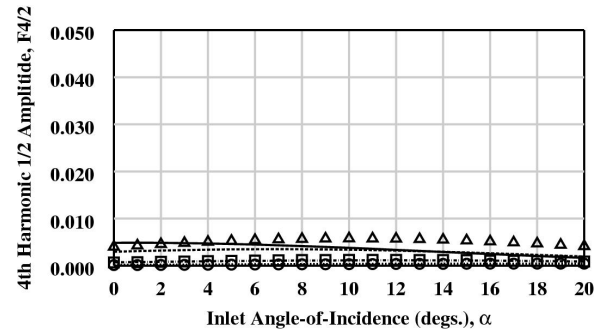


(d) 2nd Fourier Harmonic 1/2 Amplitude

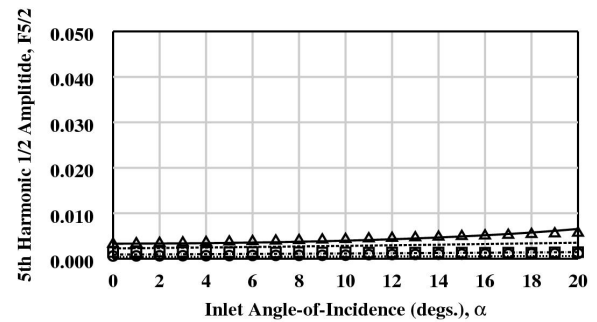
Figure (3): Comparison of “Optimal Robust” and “Optimal Adaptive” Maximum Performance inlet mission array designs



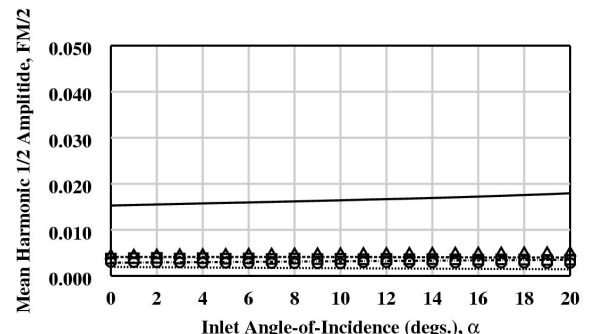
(e) 3rd Fourier Harmonic 1/2 Amplitude



(f) 4th Fourier Harmonic 1/2 Amplitude

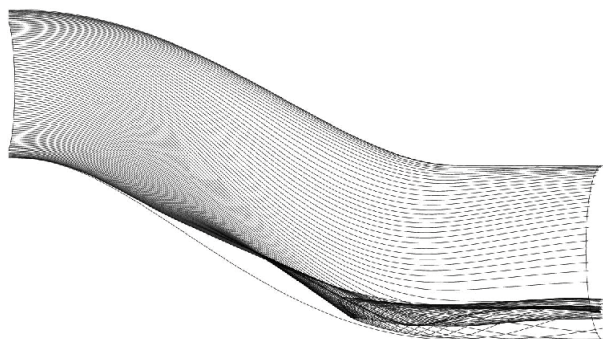


(g) 5th Fourier Harmonic 1/2 Amplitude

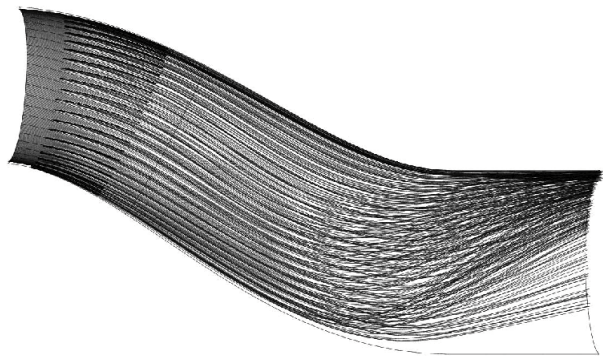


(h) Mean Fourier Harmonic 1/2 Amplitude

Figure (3): Comparison of “Optimal Robust” and “Optimal Adaptive” Maximum Performance inlet mission array designs, continued.

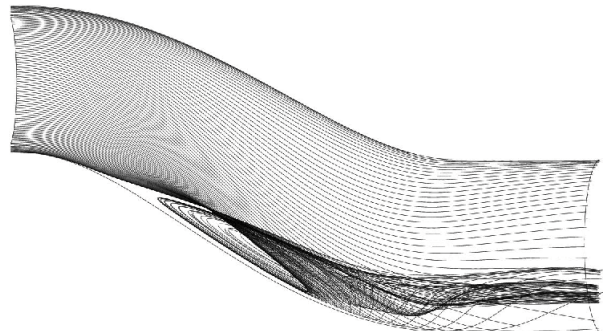


(a) Baseline Inlet

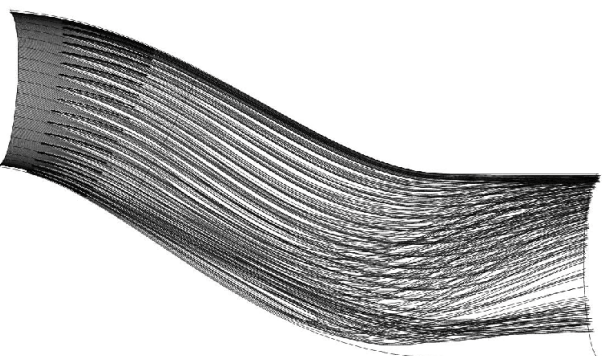


(b) Optimal Robust Max. Performance

Figure (4): Near wall inlet S-duct streamline traces, $Mt = 0.30$, $\alpha = 0.0^\circ$.

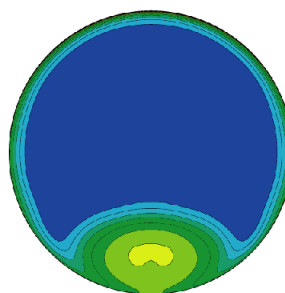


(a) Baseline Inlet

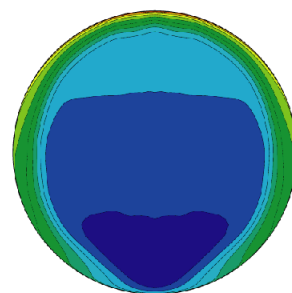


(b) Optimal Robust Max. HCF Life Expt.

Figure (5): Near wall inlet S-duct streamline traces, $Mt = 0.70$, $\alpha = 20.0^\circ$.

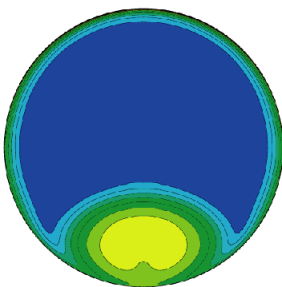


(a) Baseline Inlet

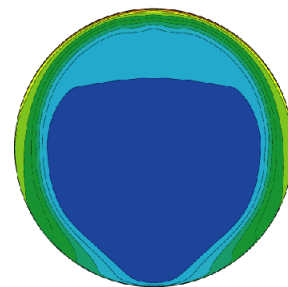


(b) Optimal Robust

Figure (6): Total pressure recovery contours, Optimal Robust Maximum Performance array, $Mt = 0.30$, $\alpha = 0.0^\circ$.

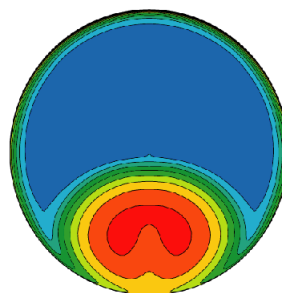


(a) Baseline Inlet

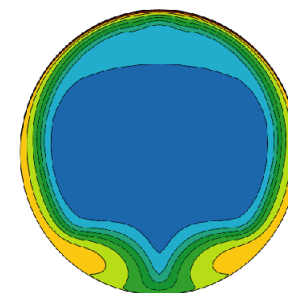


(b) Optimal Robust

Figure (7): Total pressure recovery contours, Optimal Robust Maximum Engine Stability array, $Mt = 0.50$, $\alpha = 10.0^\circ$.



(a) Baseline Inlet



(b) Optimal Robust

Figure (8): Total pressure recovery contours, Optimal Robust Maximum HCF Life Expectancy array, $Mt = 0.70$, $\alpha = 20.0^\circ$.

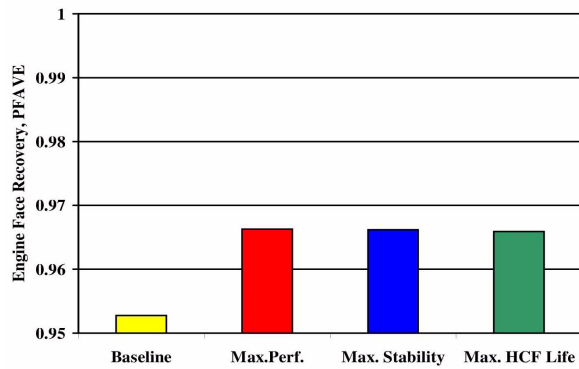


Figure (9): Effect of “Optimal Robust” array designs on inlet pressure recovery (PFAVE), $M_t = 0.70$, $\alpha = 20.0^\circ$.

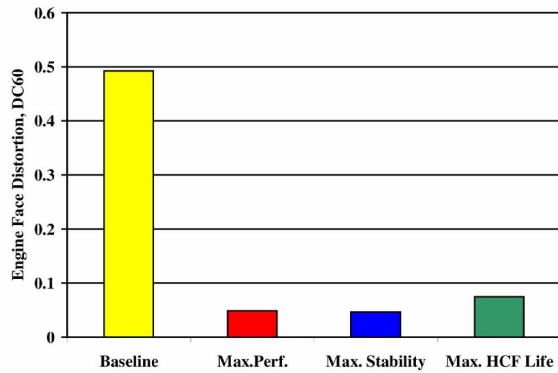


Figure (10): Effect of “Optimal Robust” array designs on engine face distortion (DC60), $M_t = 0.70$, $\alpha = 20.0^\circ$.

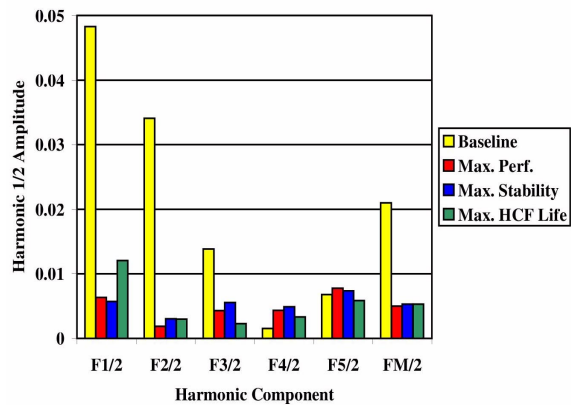


Figure (11): Effect of “Optimal Robust” array designs on the Fourier harmonic 1/2 amplitude ($F_k/2$), $M_t = 0.70$, $\alpha = 20.0^\circ$.

Response	MEAN of Sample Diff.	t*	t(0.975,8)	Comment
PFAVE	0.0	0.0	2.306	Not Diff.
DC60	0.0046	0.1734	2.306	Not Diff.
F1/2	-0.0008	0.3916	2.306	Not Diff.
F2/2	-0.0011	0.4242	2.306	Not Diff.
F3/2	-0.0006	0.6299	2.306	Not Diff.
F4/2	0.0004	0.8433	2.306	Not Diff.
F5/2	0.0	0.0	2.306	Not Diff.

Table (5): Paired t-test statistical evaluation between the (9) optimal Max. Performance cases and the (9) Max. Engine Stability cases

Response	MEAN of Sample Diff.	t*	t(0.975,8)	Comment
PFAVE	0.0008	0.3190	2.306	Not Diff.
DC60	0.0043	0.3911	2.306	Not Diff.
F1/2	0.0008	0.2600	2.306	Not Diff.
F2/2	-0.0006	0.2611	2.306	Not Diff.
F3/2	-0.0006	0.4167	2.306	Not Diff.
F4/2	0.0001	0.1421	2.306	Not Diff.
F5/2	0.0002	0.2667	2.306	Not Diff.

Table (6): Paired t-test statistical evaluation between the (9) Max. Performance cases and the (9) Max. HCF Life Expectancy cases.

Response	MEAN of Sample Diff.	t*	t(0.975,8)	Comment
PFAVE	0.0008	0.3590	2.306	Not Diff.
DC60	0.0084	0.8685	2.306	Not Diff.
F1/2	0.0156	0.4794	2.306	Not Diff.
F2/2	0.0006	0.7647	2.306	Not Diff.
F3/2	0.0	0.0	2.306	Not Diff.
F4/2	-0.0003	0.3333	2.306	Not Diff.
F5/2	0.0002	0.0544	2.306	Not Diff.

Table (7): Paired t-test statistical evaluation between the (9) Max. Engine Stability cases and the (9) Max. HCF Life expectancy cases.

REPORT DOCUMENTATION PAGE			Form Approved OMB No. 0704-0188	
Public reporting burden for this collection of information is estimated to average 1 hour per response, including the time for reviewing instructions, searching existing data sources, gathering and maintaining the data needed, and completing and reviewing the collection of information. Send comments regarding this burden estimate or any other aspect of this collection of information, including suggestions for reducing this burden, to Washington Headquarters Services, Directorate for Information Operations and Reports, 1215 Jefferson Davis Highway, Suite 1204, Arlington, VA 22202-4302, and to the Office of Management and Budget, Paperwork Reduction Project (0704-0188), Washington, DC 20503.				
1. AGENCY USE ONLY (Leave blank)		2. REPORT DATE September 2003		3. REPORT TYPE AND DATES COVERED Technical Memorandum
4. TITLE AND SUBTITLE The Role of Design-of-Experiments in Managing Flow in Compact Air Vehicle Inlets			5. FUNDING NUMBERS WBS-22-708-92-24	
6. AUTHOR(S) Bernhard H. Anderson, Daniel N. Miller, Marvin C. Gridley, and Johan Agrell				
7. PERFORMING ORGANIZATION NAME(S) AND ADDRESS(ES) National Aeronautics and Space Administration John H. Glenn Research Center at Lewis Field Cleveland, Ohio 44135-3191			8. PERFORMING ORGANIZATION REPORT NUMBER E-14158	
9. SPONSORING/MONITORING AGENCY NAME(S) AND ADDRESS(ES) National Aeronautics and Space Administration Washington, DC 20546-0001			10. SPONSORING/MONITORING AGENCY REPORT NUMBER NASA TM-2003-212601	
11. SUPPLEMENTARY NOTES Prepared for the Vehicle Propulsion Integration Symposium sponsored by the NATO Research and Technology Agency, Warsaw, Poland, October 6-9, 2003. Bernhard H. Anderson, NASA Glenn Research Center; Daniel N. Miller, Lockheed Martin Aerospace Company, Fort Worth, Texas 76101; Marvin C. Gridley, Wright Patterson Air Force Base, Dayton, Ohio 45433; and Johan Agrell, Swedish Defence Research Agency, Bromma, Sweden. Responsible person, Bernhard H. Anderson, organization code 5850, 216-433-5822.				
12a. DISTRIBUTION/AVAILABILITY STATEMENT Unclassified - Unlimited Subject Category: 07 Available electronically at http://gltrs.grc.nasa.gov This publication is available from the NASA Center for AeroSpace Information, 301-621-0390.			12b. DISTRIBUTION CODE	
13. ABSTRACT (Maximum 200 words) It is the purpose of this study to demonstrate the viability and economy of Design-of-Experiments methodologies to arrive at microscale secondary flow control array designs that maintain optimal inlet performance over a wide range of the mission variables and to explore how these statistical methods provide a better understanding of the management of flow in compact air vehicle inlets. These statistical design concepts were used to investigate the robustness properties of "low unit strength" micro-effector arrays. "Low unit strength" micro-effectors are micro-vanes set at very low angles-of-incidence with very long chord lengths. They were designed to influence the near wall inlet flow over an extended streamwise distance, and their advantage lies in low total pressure loss and high effectiveness in managing engine face distortion. The term robustness is used in this paper in the same sense as it is used in the industrial problem solving community. It refers to minimizing the effects of the hard-to-control factors that influence the development of a product or process. In Robustness Engineering, the effects of the hard-to-control factors are often called "noise", and the hard-to-control factors themselves are referred to as the environmental variables or sometimes as the Taguchi "noise" variables. Hence Robust Optimization refers to minimizing the effects of the environmental or "noise" variables on the development (design) of a product or process. In the management of flow in compact inlets, the environmental or "noise" variables can be identified with the mission variables. Therefore this paper formulates a statistical design methodology that minimizes the impact of variations in the mission variables on inlet performance and demonstrates that these statistical design concepts can lead to simpler inlet flow management systems.				
14. SUBJECT TERMS Aerodynamics; Propulsion; Fluid dynamics			15. NUMBER OF PAGES 19	
			16. PRICE CODE	
17. SECURITY CLASSIFICATION OF REPORT Unclassified	18. SECURITY CLASSIFICATION OF THIS PAGE Unclassified	19. SECURITY CLASSIFICATION OF ABSTRACT Unclassified	20. LIMITATION OF ABSTRACT	